International Journal of Scientific Engineering and Applied Science (IJSEAS) – Volume-3, Issue-5, May 2017
ISSN: 2395-3470
www.ijseas.com

TEC Proxy Index of Solar Activity for the International Reference Ionosphere IRI and its Extension to Plasmasphere IRI-Plas Model

Tamara Gulyaeva[1], Feza Arikan[2], Ljubov Poustovalova[1], Umut Sezen[2]
[1]IZMIRAN, Moscow, 142190 Troitsk, Russia
[2]Department of EEE, Hacettepe University, Beytepe, Ankara 06800, Turkey

Abstract

Recent recalibration of the sunspot number time series SSN2 has arisen a need to re-evaluate solar and ionospheric indices in the ionospheric models IRI and IRI-Plas which are developed using the predecessor SSN1 index. To improve efficiency of the ionospheric models, the ionosonde-based global IG-index used by IRI and the Global Electron Content (GEC) index used by IRI-Plas system, the new ionospheric proxy TEC-noon index is introduced based on GPS-derived Total Electron Content measurements at 288 IGS stations for 1998-2016. The regression relations are deduced between the different solar and ionospheric proxy indices smoothed by 12-month sliding window (SSN1, SSN2, F10.7, MgII, Lyman-α, $EUV_{26\text{-}34}$, $EUV_{0.1\text{-}50}$, IG, GEC, TEC_n). TEC saturation effect is detected with MgII and Lyman-α indices. Relevant subroutines are incorporated in IRI-Plas system for automatic convertion of user's predefined index to other related indices to be applied by different model procedures.

Key words: *Solar activity; Ionosphere; IRI-Plas; GIM-TEC; GEC; foF2; hmF2; W-index; Online Maps*

1. Introduction

Model is a simplified description, especially a mathematical one, of a system or process, to assist calculations and predictions (https://en.oxforddictionaries.com/definition/model).
In this context the International Reference Ionosphere (IRI) [1] and its extension to the plasmasphere (IRI-Plas) [2] are recognized as the international standard models [3-4]. IRI represents monthly averages of electron and ion densities and temperatures in the altitude range of 50 km – 2000 km. IRI-Plas – International Reference Ionosphere and Plasmasphere model includes data assimilation of Global Ionospheric Maps of Total Electron Content, GIM-TEC; the F2 layer foF2 critical frequency, proportional to NmF2 peak electron density; and the F2 layer peak height hmF2. IRI-Plas system presents modular design so that more data types can be added in the future. The system is computationally efficient capable to forecast the ionosphere state upto 24 hrs ahead of the assimilated data using the Spherical Harmonic Analysis based on 96 preceding hours. The advantage of including the plasmasphere model up to 20,200 km (GPS orbit) allows an analytical conversion by IRI-Plas of the GPS-derived Total Electron Content (TEC) to foF2 and hmF2 at each grid point of the Global Ionospheric Map, GIM-TEC. In this conversion the grid points are processed in parallel. As a result, the products of IRI-Plas system include GIM_foF2, GIM_hmF2, and GIM_W-index maps of the ionosphere variability. The aims of IRI-Plas system are to produce the good nowcasts background model dependent; accurate and actionable forecasts up to 24 hour ahead; and the long-term prediction of median ionosphere conditions.
The model output depends on what solar and ionospheric control parameters we set in the model. The 3D representation of electron density profile (vs latitude, longitude and height) is critically dependent on global ITU-R (former CCIR) model for the F2 peak plasma frequency, foF2, and M(3000)F2 factor applied for product of the peak height hmF2 values computed with IRI or IRI-Plas. The CCIR [5] mapping of foF2 and M(3000)F2 is based on using a special set of geographic functions in combination with harmonics in UT [6]. These functions are built for four levels of solar activity (12-monthly smoothed sunspot number $SSN1_{12}$ = 0, 50, 100, and 150 index units) introducing interpolation in between for any other level of solar activity.
IRI imports global effective ionospheric IG_{12} index based on ionosonde measurements of the critical frequency foF2 as a proxy of solar activity with foF2

CCIR map. Similarly, the global electron content (GEC), smoothed by the sliding 12-months window (GEC_{12}), is used as a solar proxy in the ionospheric and plasmaspheric model IRI-Plas. GEC has been calculated from global ionospheric maps of total electron content (GIM-TEC) since 1998 whereas its productions for the preceding years and predictions for the future are made with the empirical model of GEC dependence on solar activity [7].

The recent revision of the long-term sunspot number time series SSN2 over the period from 1818 to the present day [8] arise a need to re-evaluate solar and ionospheric control parameters of the ionospheric models [9]. The modified sunspot number time series SSN2 significantly differ from the original long-term series SSN1. Values of SSN2 near the solar maximum are generally higher than those of the proxy solar index of 10.7 cm microwave radio flux, F10.7, which, in turn, are on average by 60 units higher than values of SSN1 [9].

Since July, 2015, the production of the International sunspot number time series SSN1 has ceased. This reform stimulated investigations on a potential new solar activity proxy indices to be ingested into the ionospheric models [9-13]. In the present study the new ionospheric proxy index of solar activity is introduced composed from the GPS-derived Total Electron Content (TEC-noon) measurements collected at 288 IGS stations. TEC means total number of electrons on a ray path from the ground to satellite obtained in TEC units, TECU (1 TECU = 10^{16} el/m^2).

The regression relations between the different proxy indices smoothed by the12-month sliding window are deduced to be applied automatically by the IRI-Plas system which allow to adapt system to new reality of the modernization of the original set of sunspot number time series for scientific engineering and telecommunication issues.

2. Relations between the different solar proxies.

The ionospheric global IG index was obtained [14] by adjusting the CCIR [5] model for foF2 to the noontime measurements of several reference ionosonde stations. This is achieved by changing the $SSN1_{12}$ index that describes the solar activity variations in the CCIR model. The final step is taking the average over all stations to generate the global IG index. It is produced and distributed by the UK Solar System Data Centre in Slough, England. The original index was produced based on 11 reference stations, however not all of these stations have remained in operation or continued to be able to share their data. Currently the index is determined with 4 reference stations: two from the Southern hemisphere (Port Stanley, U.K.,, and Canberra, Canada) and two from the Northern hemisphere (Kokubunji, Japan, and Chilton, U.K.). This has limited the reliability of this index in representing the global ionospheric conditions, nevertheless it is still superior to the SSN1 and F10.7 indices in describing the solar cycle changes in the F-region ionosphere. In IRI the 12-month running mean IG_{12} is used with the CCIR [5] foF2 model and therefore has a strong impact on the whole electron density profile since it is normalized to the F2 peak and since the ionosphere reaches its highest densities at the F2 peak.

Due to above limitations of IG_{12} index, the global electron content (GEC), smoothed by the sliding 12-months window (GEC_{12}), is used as a solar proxy in the ionospheric and plasmaspheric model IRI-Plas. However, the GPS based GEC index depends on its temporal coverage (since 1998 to present) and its extrapolation in time [7]. Its production by IRI-Plas system with the CCIR maps depends on SSN1 input which itself become a problem after re-calibration since 2015.

TEC-noon proxy index of solar activity is developed here for the first time in literature based on GPS-TEC measurements at 288 IGS stations listed at http://www.izmiran.ru/ionosphere/weather/tec/. These TEC data cover the period since mid-1998 to present and are refreshed every day. First, we produce monthly median for local noon at each IGS station, then apply 12-months smoothing to global average of the monthly medians at all stations, and designate the results as the ionospheric proxy index TEC_{12}.

Fig. 1 illustrates 12-monthly smoothed TEC_{12} index obtained in TECU for 1999-2015, $SSN1_{12}$ and $SSN2_{12}$ time series for the same period.

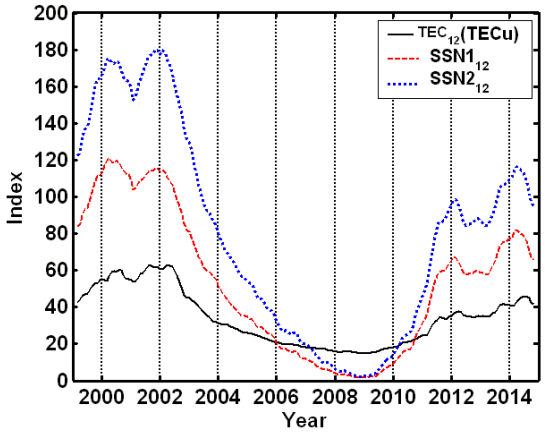

Fig. 1. Solar sunspot numbers and TEC_{12} ionospheric index observed from 1999 to 2015.

Clear difference between absolute values of three data set is seen but their variation is synchonised according to solar activity (SA) cycle which shows similar behaviour from SA minimum to maximum. Relation between $SSN1_{12}$ and $SSN2_{12}$ is established in [9] as

$$SSN1_{12} = 0.7 \times SSN2_{12} \quad (1)$$

It is worth to find out relation between TEC_{12} index and the ionosonde based IG_{12} index. Their relation is plotted in Fig. 2.

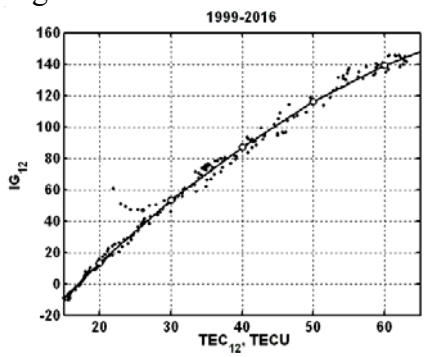

Fig. 2. The ionospheric index IG_{12} calculated from ionosonde network measurements of f_0F2 for the midday against the noon TEC_{12}. The curve is the model by Eqs. (2-3).

Fig. 2 demonstrates the saturation of the peak electron density NmF2 (proportional to foF2) which is well known phenomenon in the ionosphere when the electron density reaches the limit and stops increasing with further increasing of solar activity [1, 9, 13]. The saturation of IG_{12} with growing TEC_{12} is clearly seen in Fig. 2. However, it is not clear from these data if TEC measured through altitudes from 65 to 20,200 km (GPS orbit) suffer the saturation with growing solar activity similar to foF2 measured within 250-400 km above the Earth. The dependence between two indices can be expressed by the second-order polynomial (the solid curve in Fig. 2):

$$TEC_{12} = 0.0008 \times IG_{12}^2 + 0.1951 \times IG_{12} + 17.1819 \quad (2)$$

$$IG_{12} = -0.0276 \times TEC_{12}^2 + 5.3533 \times TEC_{12} - 82.5499 \quad (3)$$

Implementation of Eq. (2) allows modelling TEC_{12} variation for the total period of availability of IG_{12} index from 1958 to present and its prediction to the end of 2019. The results are plotted in Fig. 3 including IG_{12} index during 1958-2019, TEC_{12} model and TEC_{12} observations.

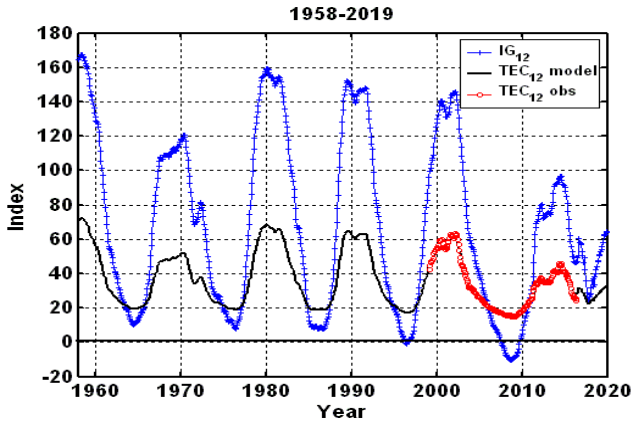

Fig. 3. Time series of IG12 index during 1958-2019, TEC12 modeling results and TEC12 observations. Metrics of TEC_{12} is TECU.

Now a regression model of TEC_{12} index on $SSN1_{12}$ could be produced. This process is illustrated in Fig. 4 where the regression between $SSN1_{12}$ and TEC_{12} (as observed in TECU) is indicated by black line with circles along the lower set of points expressed by Eq. (4):

$$TEC_{12}\ obs = 0.3875 \times SSN1_{12} + 13.5411 \quad (4)$$

Scaling TEC_{12} observed to TEC_{12} proxy index corresponding to metrics of $SSN1_{12}$ is made with Eq. (5) as shown with the upper set of ponts in Fig.2:

$$TEC_{12}\,proxy = 2.4112 \times TEC_{12}\,obs - 31.3456 \quad (5)$$

Regression of TEC_{12} proxy index on $SSN1_{12}$ is plotted by dashed line along the upper set of points in Fig. 4 and expressed by the model Eqs. (6-7):

$$TEC_{12} = 0.9359 * SSN1_{12} + 1.71 \quad (6)$$

$$SSN1_{12} = 1.0385 \times TEC_{12} - 0.2864 \quad (7)$$

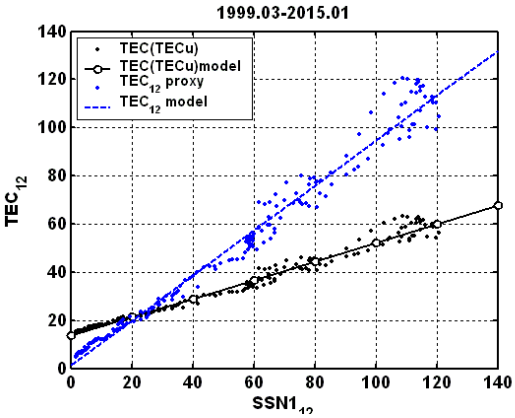

Fig. 4. Regression between TEC_{12} index observed in TECU (lower set of data) and TEC_{12} proxy index scaled to $SSN1_{12}$ values (upper set).

Time series of $SSN1_{12}$, observed before mid-2015 and calculated afterwards with Eq. (1), new $SSN2_{12}$ index, and TEC12 proxy index modelled with Eq. (6) substituting $SSN1_{12}$ index for the solar cycles 17 to 24 (1930-2019) are plotted in Fig. 5. TEC_{12} proxy index is close to $SSN1_{12}$ index except for the minor differences near the peak of the solar cycles. TEC_{12} has the advantage for driving the ionospheric models because of its permanent observations and online availability from 1998 onwards, so it can be used for production of $SSN1_{12}$ index with Eq. (7) due to its absence since mid-2015.

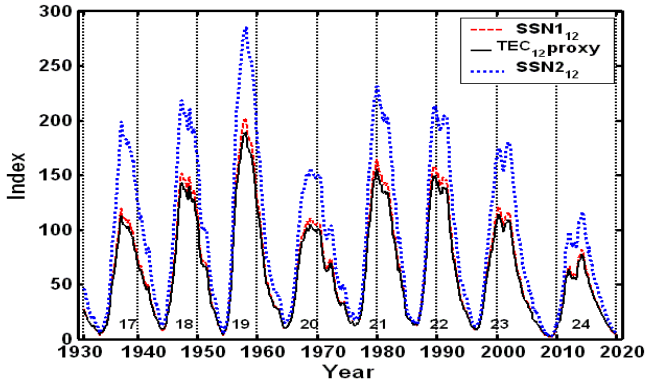

Fig. 5. Time series of $SSN1_{12}$, $SSN1_{12}$, solar sunspot numbers and modeling results of TEC_{12} proxy indices during 1930-2019.

The regression relationship between SSN1 and F10.7 employed in the IRI and IRI-Plas models held until 2000, but after 2001 it changed [15] so that after 2001 $F10.7_{12}$ also began to significantly exceed $SSN2_{12}$ [9]. To provide mutually consistent solar activity proxies in IRI and IRI-Plas model subroutines which rely on either of above two indices, the regression relashipship between $F10.7_{12}$ index and $SSN1_{12}$ index specified with CCIR maps is updated below using these indices from 1948 to 2019. Here their observations and prediction for 2016-2019 and $SSN1_{12}$ model of Eq. (1) from mid-2015 onwards are included (Fig. 6). The regression model for these solar indices are expressed by Eqs. (8-9):

$$F10.7_{12} = 0.9066 \times SSN1_{12} + 62.6645 \quad (8)$$

$$SSN1_{12} = 1.0760 \times F10.7_{12} - 65.7817 \quad (9)$$

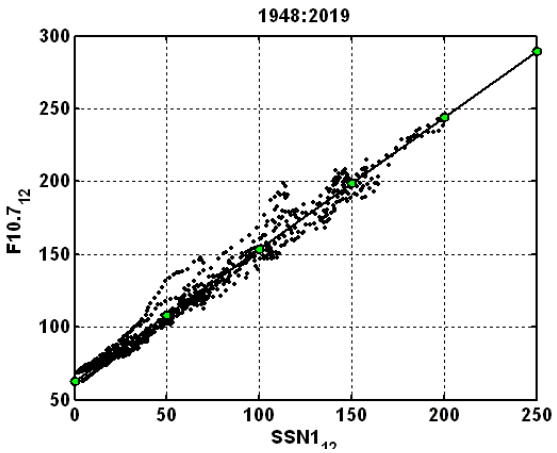

Fig. 6. Regression relashinships between $F10.7_{12}$ index and $SSN1_{12}$ values during 1948 to 2019.

The solar EUV irradiance represents the main ionization source of the F2 ionospheric layer [16]. In particular, a decrease of ~15% in the EUV solar radiation has been found for the minimum of solar cycle 23/24 as compared to the previous one, which explains the lower values of foF2 observed by ionospheric stations all around the world [17].

The considerable difference in foF2 – EUV data relation in the solar cycle SC 24 characterizing the solar EUV radiation as compared with SC 23 is illustrated in Fig. 7. Here 12-month smoothed noon foF2 measurements at Moscow, Chilton and Canberra are plotted against EUV_{12} at the wavelengths 24-36 nm and 0.1-50 nm.

This picture confirms the earlier observation that the long–term relation between the EUV irradiance and F10.7 has changed markedly since around 2006, with EUV levels decreasing more than expected if compared to the F10.7 index [17- 18]. This could be ascribed to a potential degradation of the SOHO/SEM instrument, which would cause a drift of solar measurements and a consequent overestimation of the EUV[0.1–50] and EUV[24-36] irradiance [17, 19]. By this virtue the EUV indices should be disregarded as the solar parameters driving the ionospheric models.

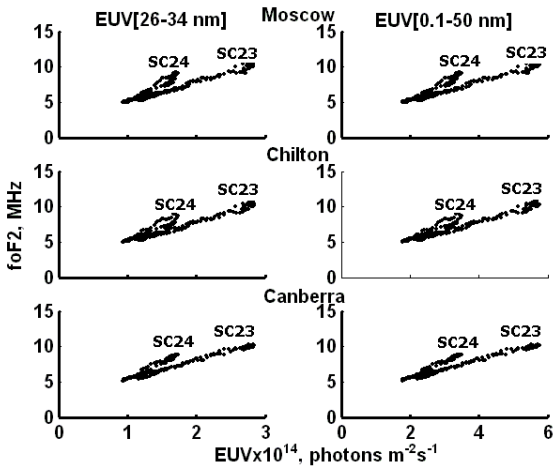

Fig. 7. 12-month smoothed noon foF2 measurements at Moscow (55°N, 37°E), Chilton (52°N, 1°W) and Canberra (35°S, 149°E) against EUV_{12} at the wavelengths 24-36 nm and 0.1-50 nm for 23rd and 24th solar cycles.

The core–to–wing ratio of the magnesium ion h and k lines at 279.56 and 280.27 nm is also a good indicator of the solar chromospheric activity, and is a useful proxy for solar irradiance in the UV and EUV wavelengths [20]. Called MgII core–to–wing index, it is calculated by taking the ratio between the highly variable chromospheric lines and the weakly varying photospheric wings [21]. *Mg II* data were downloaded from the free on–line database of Institut fur Umweltphysik - Universitat Bremen (http://www.iup.uni–bremen.de/gome/gomemgii.html), and are available from November, 1978 to present (courtesy: Mark Weber). Its 12-month smoothed relation with TEC_{12} index is plotted in Fig. 8a.

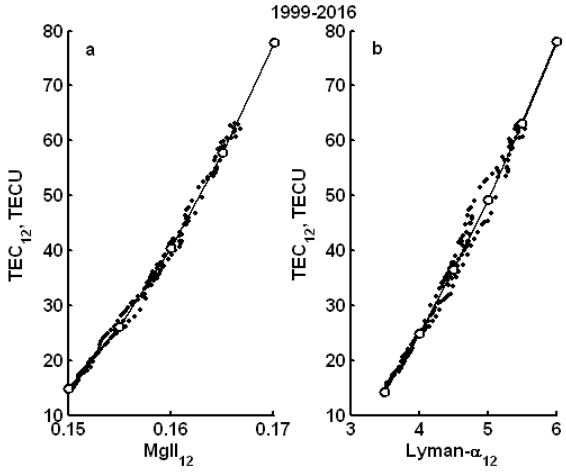

Fig. 8. TEC_{12} relations with (a) MgII core–to–wing index; (b) Lyman–α emission index.

The hydrogen Lyman–α emission at 121.6 nm represents the strongest single line in the UV band, and has been measured for decades by rockets, the Atmosphere Explorer (AE) series of satellites, the Solar Mesosphere Explorer (SME), the Upper Atmosphere Research Satellite (UARS), the Thermosphere Ionosphere Mesosphere Energetics

and Dynamics (TIMED), and the Solar Radiation and Climate Experiment (SORCE) missions [21]. A composite index is based on a careful intercalibration of these measurements and the corresponding gaps are filled using correlation relations with $F10.7$ and MgII indices [22]. Fig. 8b reproduces relation of TEC_{12} index with Lyman–α.

The effect of TEC_{12} saturation is best demonstrated with MgII and Lyman–α indices. Unlike to relations with SSN1 (Fig. 4), a linear fit is not suitable for the both sub-plots of Fig. 8. Due to effect of TEC saturation, the quadratic polynomial relation is best suitable for fitting the curves for TEC_{12} relation with these two solar indices:

$$TEC_{12} = 5{,}9195 \times MgII_{12}^2 - 1{,}5781 \times MgII_{12} + 1050 \quad (10)$$

$$MgII_{12} = -0.0231 \times 10^{-4} \times TEC_{12}^2 + 0.000511 \times TEC_{12} + 0.1432 \quad (11)$$

$$TEC_{12} = 2.1473 \times L\alpha_{12}^2 + 5.1484 \times L\alpha_{12} - 30.1336 \quad (12)$$

$$L\alpha_{12} = -0.000179 \times TEC_{12}^2 + 0.05393 \times TEC_{12} + 2.776 \quad (13)$$

Thus the regresion models are provided for all solar and ionospheric indices under consideration except for EUV at the wavelengths 24-36 nm and 0.1-50 nm. The user of IRI and / or IRI-Plas code should select one "basic' index preferable for his/her task which is entered authomatically by the system. Then the relevant sunroutines would relate this basic index to all other indices foreseen by the different modules of system to keep the output results mutually consistent.

3. Conclusions

Recent recalibration of the sunspot number time series SSN2 presents challenge for the ionospheric models IRI and IRI-Plas which are developed using the predecessor SSN1 index. The ionosonde-based ionospheric global IG-index incorporated into IRI and the Global Electron Content (GEC) index used by IRI-Plas system are complemented in the present study with the Total Electron Content (TEC-noon) index scaled to the pre-defined SSN1 time series based on GPS-derived TEC measurements at 288 IGS stations.

Earlier studies of long-term relations of different solar and ionospheric proxy indices have revealed that the best results for the ionospheric modeling are obtained with the *MgII* index [10-13]. Our investigation appears also to point out TEC saturation effect recognised for the first time with MgII and Lyman-α indices. So these solar indices and the new introduced the ionospheric TEC_{12} index are the best candidates to be entered into IRI-Plas system.

The regression relations are deduced between the different solar and ionospheric proxy indices smoothed by 12-month sliding window ($SSN1_{12}$, $SSN2_{12}$, $F107_{12}$, MgII, Lyman-α, IG_{12}, GEC_{12}, TEC_{12}). Relevant subroutines are incorporated in IRI-Plas system for automatic convertion of user's predefined index to other related indices used by different model procedures. The further validation of the model with new solar proxies and new databases is open for discussion by the ionospheric modeller and model users.

Acknowledgments

TEC data are provided by the Jet Propulsion Laboratory of California Institute of Technology (JPL) at ftp://sideshow.jpl.nasa.gov/pub/iono_daily/. This study is partly supported by TUBITAK EEEAG 115E915.

References.

[1] D. Bilitza, D. Altadill, V. Truhlik, V. Shubin, I. Galkin, B. Reinisch, X. Huang. "International Reference Ionosphere 2016: from ionospheric climate to real-time weather predictions", Space Weather, Vol. 52, No. 2, 2017, pp. 418-429.

[2] T. L. Gulyaeva, F. Arikan, M. Hernandez-Pajares, I. Stanislawska. "GIM-TEC adaptive ionospheric weather assessment and forecast system", J. Atmos. Solar-Terr. Phys., Vol. 102, 2013, pp. 329-340.

[3] T. L. Gulyaeva and D. Bilitza. "Towards ISO Standard Earth Ionosphere and Plasmasphere

Model", in: "New Developments in the Standard Model", edited by R.J. Larsen, , NOVA, Hauppauge, New York, 2012, pp. 1-39.

[4] F. Arikan, U. Sezen, T. L. Gulyaeva, O. Cilibas. "Online, Automatic, Ionospheric Maps: IRI-PLAS-MAP", Adv. Space Res., Vol. 55, No. 8, 2015, pp. 2106-2113.

[5] CCIR Atlas of Ionospheric Characteristics. *Comite Consultatif International des Radio Communications Rep. 340*. Geneve, International Telecommunication Union, 1983.

[6] W. B. Jones, R. M. Gallet. "Representation of diurnal and geographical variations of ionospheric data by numerical method", Telecomm. J., Vol. 29, 1962, pp. 129; Vol. 32, 1965, pp. 18.

[7] T. L. Gulyaeva, I. S. Veselovsky. "Imaging Global Electron Content backwards in time more than 160 years ago", Adv. Space Res., Vol. 53, No. 3, 2014, pp. 403–411.

[8] F. Clette, L. Svalgaard, J. M. Vaquero, E. W. Cliver. "Re-visiting the sunspot number: a 400-year perspective on the solar cycle", Space Sci. Rev., Vol. 186, No. 1, 2014, pp. 35–103.

[9] T. Gulyaeva. "Modification of the solar activity indices in the International Reference Ionosphere IRI and IRI-Plas models due to recent revision of sunspot number time series", Solar-Terr. Phys., Vol. 2, No. 3, 2016. pp. 59-68.

[10] K. Hocke. "Oscillations of global mean TEC". J. Geophys. Res., Vol. 113, A04302, 2008. DOI:10.1029/2007JA012798.

[11] T. Maruyama. "Solar proxies pertaining to empirical ionospheric total electron content models", J. Geophys. Res., Vol. 115, A04306, 2008. DOI:10.1029/2009JA014890.

[12] Y. Chen, L. Liu, W. Wan. "The discrepancy in solar EUV–proxy correlations on solar cycle and solar rotation timescales and its manifestation in the ionosphere. J. Geophys. Res., Vol. 117, 2012, pp. 2-13. DOI:10.1029/2011JA017224.

[13] L. Perna, M. Pezzopane. "foF2 vs Solar Indices for the Rome station: looking for the best general relation which is able to describe the anomalous minimum between cycles 23 and 24. J. Atmosph. Solar-Terr. Phys., 2016, DOI:10.1016/j.jastp.2016.08.003.

[14] R. Liu, P. Smith, J. King. "A new solar index which leads to improved foF2 predictions using the CCIR atlas", Telecomm. J., Vol. 50, 1983, pp. 408-414.

[15] R. Lukianova, K. Mursula. "Changed relation between sunspot numbers, solar UV/EUV radiation and TSI during the declining phase of solar cycle 23". J. Atmos. Solar-Terr. Phys., Vol. 73, No. 2–3, 2011, pp. 235–240.

[16] W. K. Tobiska. "Current status of solar EUV measurements and modeling". Adv. Space Res., Vol. 18, 1996. pp. 3–10. DOI:10.1016/0273–1177(95)00827–2.

[17] Y. Chen, L. Liu, W. Wan. "Does the F10.7 index correctly describe solar EUV flux during the deep solar minimum of 2007–2009?" J. Geophys. Res. Space Phys. Vol. 116, 2011, pp. 1–6. DOI:10.1029/2010JA016301.

[18] J. T. Emmert, J. L. Lean, J. M. Picone. "Record–low thermospheric density during the 2008 solar minimum". Geophys. Res. Lett., Vol. 37, L12102, 2010. DOI:10.1029/2010GL043671.

[19] S. R. Wieman, L. V. Didkovsky, D. L. Judge. "Resolving Differences in Absolute Irradiance Measurements Between the SOHO/CELIAS/SEM and the SDO/EVE". Sol. Phys., Vol. 277, 2014, pp 285–303. DOI:10.1007/978–1–4939–2038–9_18.

[20] R. A. Viereck, , L. E. Floyd, P. C. Crane, T. N. Woods, B. G. Knapp, G. Rottman, M. Weber, L. C. Puga, M. T. DeLand. "A composite Mg II index spanning from 1978 to 2003". Space Weather, Vol. 2, S10005, 2004. DOI:10.1029/2004SW000084.

[21] S. C. Solomon, L. Qian, A. G. Burns. "The anomalous ionosphere between solar cycles 23 and 24". J. Geophys. Res. Space Phys. Vol. 118, 2013, pp. 6524–6535. DOI:10.1002/jgra.50561.

[22] T. N. Woods, W. K. Tobiska, , G. J. Rottman, J. R. Worden. "Improved solar Lyman α irradiance modeling from 1947 through 1999 based on UARS observations". J. Geophys. Res., Vol. 105, 27195, 2000. DOI:10.1029/2000JA000051.